

MACROPARTICLE SIMULATION OF STOCHASTIC COOLING

ANDREI GERASIMOV

*Fermi National Accelerator Laboratory,
P.O. Box 500, Batavia, IL 60510, USA**

(Received 9 December 1994; in final form 13 June 1995)

The feasibility of the macroparticle simulation of stochastic (momentum) cooling is discussed. A computationally effective algorithm for simulating the particle dynamics is proposed. The scaling laws for the number of particles and cooling system bandwidth are numerically checked. Results of simulation of the momentum stacking in a simplified model are presented, indicating that reproducing 3 orders of magnitude in the density variation is easily achievable.

KEY WORDS: Stochastic cooling

1 INTRODUCTION

The performance of the \bar{p} accumulating rings is usually simulated by numerically solving the Fokker-Planck (FP) equation for the momentum cooling.¹ This approach however can not be easily extended to account for many real-life complications, particularly the two-way transverse-longitudinal coupling due to the finite betatron size at the pickup. Indeed, the computational complexity of the Fokker-Planck solvers grows with the dimensionality of the space p as N^p (N being the number of points on the grid), so going from $p = 1$ to $p = 2$ in the situation when the code for $p = 1$ case is already quite slow,² would most likely be not feasible. Likewise, the more complicated time-dependent boundary conditions that are met, e.g., in the RF injection process for the momentum stacking of antiprotons,³ are hard to incorporate into the Fokker-Planck models and particularly into already existing codes. An alternative approach to stochastic cooling simulation that seems more flexible was suggested by V. Visnjic⁴ and can be described as the macroparticle simulation using the discrete particles and the time-domain response functions of the pickup-kicker (PU-K) circuits. Since it is not possible to use the realistic number of \bar{p} that is about 10^{10} , one needs an appropriate scaling law to extrapolate from the results with a smaller number of particles. In this note, we present such a scaling law for an idealized momentum-

*Operated by the Universities Research Association, Inc. under contract with the U.S. Dept. of Energy.

cooling system (without coupling to transverse dynamics). In addition, another useful scaling law that allows to change the bandwidth, is derived. An efficient macroparticle time dynamics algorithm is obtained, and some preliminary results of simulation are presented. The feasibility of macroparticle simulation is established by numerically testing the scaling laws. The new method provides an alternative way of simulating stochastic cooling systems. The momentum stacking simulation with fully coupled transverse-longitudinal degrees of freedom has been already carried out and will be published separately.³

2 THEORY AND ALGORITHMS

2.1 Scaling laws for the Fokker-Planck model

We base our discussion on the theoretical derivation of Reference 5. (BL). The Fokker-Planck model of the evolution of momentum distribution function $\Psi(x, t)$ (with x for momentum deviation from the reference particle $x = E - E_0$ and t for time) is given by (BL50) as:

$$\frac{\partial \Psi}{\partial t} = -\frac{\partial}{\partial x} \left[F(x, t)\Psi - D(x, t)\frac{\partial \Psi}{\partial x} \right] \quad (1)$$

where the “damping” $F(x, t)$ and “diffusion” $D(x, t)$ are:

$$F(x, t) = \sum_l \frac{G_l(x)}{\epsilon_{-l}(x, t)} \quad (2)$$

$$D(x, t) = \Psi(x, t) \frac{N\pi}{\left| \frac{d\omega}{dx} \right|} \sum_l \frac{1}{|l|} \left| \frac{G_l(x)}{\epsilon_{-l}(x, t)} \right|^2 + D_{th}(x) \quad (3)$$

where $\omega(x)$ is the revolution frequency dependence on momentum, G_l and ϵ_l are respectively the gain and the signal suppression factor at harmonic l of the revolution frequency. The latter quantity is defined by:

$$\epsilon_{\pm|l|}(x, t) = 1 + \frac{N}{|l|} \int_{\eta \rightarrow 0_+} dx_1: \frac{G_{\pm|l|}(x_1) \frac{\partial \Psi(x_1, t)}{\partial x_1}}{\eta \pm i(\omega(x) - \omega(x_1))} \quad (4)$$

where N is the total number of particles. The distribution function $\Psi(x, t)$ is normalized $\int dx \Psi(x, t) = 1$. The diffusion intensity $D_{th}(x)$ is caused by the thermal noise in the pick-ups and the electronic circuits and is given by:

$$D_{th}(x) = \pi \left(\frac{l\omega}{2\pi} \right)^2 \sum_l \frac{P(l\omega(x))}{\epsilon_{-l}(x)} \quad (5)$$

where $P(\Omega)$ is the noise power density. The gain harmonics $G_l(x)$ are defined as $G(l\omega(x), x)$ of the general gain function $G(\Omega, x)$. In the expression (4), the Palmer cooling technique is implied, since the gain G stands under the integration.⁵ Notice that the gain harmonics G_l are generally complex quantities as they include the phase factors from the “unwanted mixing” between the pickup and the kicker.⁵ Thus, the Fokker-Planck models described below and the scaling transformation fully account for that effect.

The crucial issue for the possibility of the macroparticle simulation is the existence of the scaling laws for the Fokker-Planck equation (1) that would allow to reduce the total number of particles N . It is resolved positively by identifying the (scaling law) transformation:

$$\begin{aligned} N' &= \frac{N}{k} \\ G'_l(x) &= kG_l(x) \\ P'_l(x) &= kP_l(x) \\ t' &= \frac{t}{k} \end{aligned} \tag{6}$$

that leaves the FPE (1) invariant. It should be noted that the flux $J = F\Psi - D\frac{\partial\Psi}{\partial x}$ is invariant under the transformation (6) together with the “screening factors” ϵ_l . The meaning of the transformation (6) in terms of the cooling rate is that by decreasing (increasing) the number of particles by a factor k and simultaneous increasing (decreasing) of the gain by the same factor, the cooling rate is increased by the factor k . Notice here that the FPE invariance is a stronger property than the cooling time invariance, since the latter may change as the cooling progresses while the former can not.

The transformation (6) allows us to reduce the number of particles for simulation purposes to what is numerically practical. It is important to realize however that this is only true when one extra condition is met: the number of particles within a “sample” has to be large, i.e.:

$$\frac{N}{WT} \gg 1 \tag{7}$$

where W is the bandwidth of the cooling system and T is the revolution period. Indeed, the condition (7) guarantees the wide separation of the coherent and incoherent (cooling) time scales that justifies the truncation of the BBGKY hierarchy in order to derive the FPE.⁵

The necessity to satisfy the condition (7) makes one to look for some other scaling laws that would allow to reduce the bandwidth and push down the number of particles still further. Indeed, in the example of the Fermilab Accumulator Ring the bandwidth of the momentum stacking system extends up to ~ 4500 revolution frequencies, so one would still need about 20000–100000 particles to satisfy the condition (7). That can be too many for practical application, as we show in the next section.

The transformation of the required type that we propose to use is:

$$\begin{aligned} G'_l(x) &= G_{Rl}(x) \\ \omega'(x) &= \omega_0 + R(\omega(x) - \omega_0) \\ P'_l(x) &= \frac{P_l(x)}{R} \\ t' &= Rt \end{aligned} \tag{8}$$

where ω_0 is the revolution frequency of the reference particle $\omega_0 = \omega(0)$, while the index Rl is understood as the integer part $[Rl]$. The transformation (8) is defined for any positive R both larger and smaller than unity. Unlike the situation with the transformation (6), the FPE will be invariant under the “bandwidth transformation” (8) only approximately and only when both the original and the transformed bandwidths are large, $WT \gg 1$, $WT/R \gg 1$. Indeed, one can easily see that the signal suppression factors are transformed as $\epsilon'_l = \epsilon_{Rl}$. Moreover, if the gain harmonics G_l change slowly, as a function of l , from $l_{\min} \sim 0.5WT$ to $l_{\max} \sim WT$, the summation over l in the formulas (2) and (3) for the damping and diffusion intensities can be substituted by integration, producing:

$$F'(x) = \sum_l \frac{G_{Rl}}{\epsilon_{-Rl}} \approx \frac{1}{R} \sum_l \frac{G_l}{\epsilon_{-l}} = \frac{F(x)}{R} \tag{9}$$

and similarly $D'(x) = D(x)/R$. When $R > 1$, the transformation (8) reduces the bandwidth and the cooling slows down proportionately. Notice that the flux J is transformed as $J' = J/R$.

Finally, one more transformation that rescales the gain without a change in the number of particles is:

$$\begin{aligned} G'_l(x) &= k_1 G_l(x) \\ \omega'(x) &= \omega_0 + k_1(\omega(x) - \omega_0) \\ P'_l(x) &= k_1 P_l(x) \\ t' &= \frac{t}{k_1} \end{aligned} \tag{10}$$

The flux J for this transformation scales as $J' = k_1 J$.

The three transformations (6), (8) and (10) allow to adjust independently three parameters, e.g. gain strength, bandwidth and frequency spread. All three transformations should be implemented to increase the speed of the macroparticle simulation, as is discussed in the following sections. The transformations affect both the real and imaginary parts of the gain

and fully account, in particular, for the “unwanted mixing” between the pickup and the kicker.

2.2 Dynamics with cooling: efficient algorithms

The longitudinal equations of motion in a ring with one PU and one K can be defined as:

$$\begin{aligned}\dot{x}_i &= -q\delta_{2\pi}(\theta_i - \theta^K) \\ \dot{\theta}_i &= \omega(x_i) \\ \ddot{q} &= \sum_i H(x_i) \delta_{2\pi}(\theta_i - \theta^{PU}) + \int_0^\infty d\tau F(\tau)q(t - \tau)\end{aligned}\tag{11}$$

where x_i is the relative energy of the i -th particle $x_i = E_i - E^0$, θ_i is the azimuthal coordinate, and θ^K, θ^{PU} are the azimuthal locations of respectively the PU and the K. The quantity $q(t)$ is the voltage at the kicker as a function of time, the function $H(x)$ describes the position sensitivity of the PU in the Palmer cooling method,⁵ and the retarding kernel $F(\tau)$ accounts for the net effect of amplifiers and filters. The time-domain dynamics (11) can be related to the more conventional frequency-domain calculations⁵ by using the fast-time (unperturbed) oscillations $\theta_i = \theta_{i0} + \omega(x_i)t$, yielding:

$$q(t) = \sum_{l=-\infty}^{\infty} \sum_i \frac{H(x_i) e^{il(\theta_{i0} + \omega(x_i)t - \theta^{PU})}}{\omega^2(x_i) - F_\omega(\omega(x_i))}\tag{12}$$

where $F_\omega(\omega)$ is the Fourier image of $F(\tau)$. The gain $G(\Omega, x)$ is then:

$$G(\Omega, x) = \frac{H(x) e^{i(\theta^K - \theta^{PU})}}{\Omega^2 - F_\omega(\Omega)}\tag{13}$$

and $G_l(x) = G(l\omega(x), x)$. The form (13) can describe both the Palmer cooling when the denominator is nonzero at $\Omega = l\omega_0$ while $H(0) = 0$ and the filter cooling, when $H(0) \neq 0$ and $F_\omega(l\omega_0) = \infty$.

In time domain, the dynamical solution of the equation for q (11) can be presented as:

$$q(t) = \sum_{k=1}^{\infty} \sum_i \bar{G}(t - \tilde{t}_k^i, \tilde{x}_k^i)\tag{14}$$

where i is the particle number, \tilde{t}_k^i is the moment of crossing the PU number k (counted from moment t backwards), and \tilde{x}_k^i is the momentum x_i at that crossing. The Green function $\bar{G}(t, x)$ is the Fourier transform of the gain $G(\Omega, x)$.

The typical time dependence of the Green function $\bar{G}(t, x)$ is shown in Figure 1 (light curve).

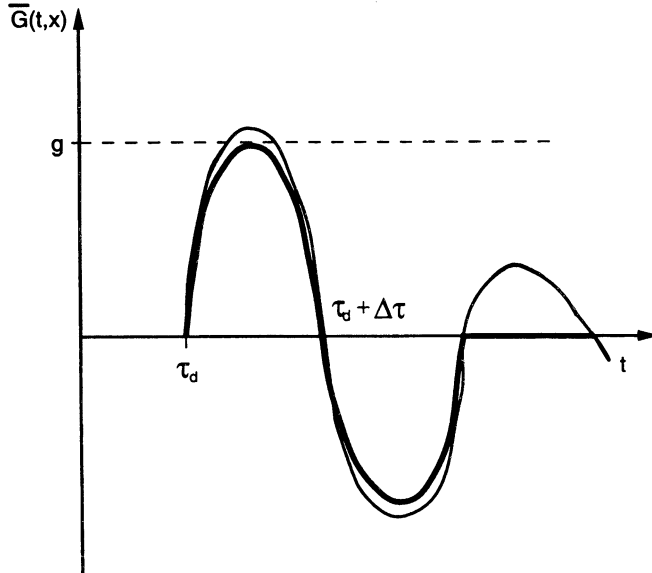


FIGURE 1: Typical time dependence of the Green function $\bar{G}(t, x)$ (light curve). Fat curve is an “idealized” dependence that is used in the simulation code. Upper and lower “humps” on the fat curve are parabolic.

The Green function $\bar{G}(t, x)$ is zero for $\tau < \tau_d$, where τ_d is the PU-K delay time. The width of the impulse $\Delta\tau = \tau_{\max} - \tau_d$ is determined by the bandwidth $W = 2\pi/\Delta\tau$. Though for any real filter the “tail” of the Green function is nonzero at $t > \tau_{\max}$, for the purpose of our macroparticle simulation we will consider an approximation of zero $\bar{G}(x, t)$ for $t > \tau_{\max}$, substituting thus the real Green function by the one with the “tail cut-off”, as shown in Figure 1. This approximation allows one to have only a finite (and relatively small) number of particles that have crossed the PU to contribute to the K voltage at any given moment of time. More specifically, there will be only about $N_s \sim N\Delta\tau/T$ particles at their latest PU crossing moments of time $\tilde{t}_1^i = \tilde{t}^i$ that contribute to the sum (14).

Dynamical system (11) can be cast in the form of the mapping in discrete time steps of the order of the revolution period. The most computation-efficient ways of choosing the time step of the mapping are described in Reference 6. The simulation code that is described below utilizes the mapping of that kind.

2.3 Schottky spectra

One of the most important diagnostic tools in the real experimental environment are the Schottky signal monitors.^{1,7} In order to be able to compare the simulation data with the experimental one, one needs to calculate the Schottky spectra in simulation. The Schottky spectrum $S(\omega)$ can be calculated by using the definition:

$$S(\omega) = \lim_{T_s \rightarrow \infty} \int_0^{T_s} dt e^{i\omega t} K(t) \quad (15)$$

where the auto-correlation function $K(\tau)$ is defined as:

$$K(\tau) = \lim_{T_k \rightarrow \infty} \frac{1}{T_k} \int_0^{T_k} dt I(t) I(t + \tau) \quad (16)$$

The PU current $I(t)$ is the sum of the δ -functional impulses from each particle traversing the PU at $\theta = 0$:

$$I(t) = \sum_i \omega(x_i(t)) \delta(\theta_i(t)) \quad (17)$$

where $\delta(\theta)$ is the 2π -periodic delta-function and we assumed a momentum-insensitive PU. In simulation, the integrations in the formulas (15) and (16) are done in the finite ranges T_s and T_k . Within given computational resources, the ratio N/T_k and parameters T_k , T_s have to be chosen optimally in order to minimize the fluctuations of the Schottky spectra. The optimal choice of T_s , T_k and the fluctuations of the Schottky spectra are described in Reference 6.

3 SIMULATION CODE AND PRELIMINARY RESULTS

The code that implements the algorithm of the preceding section was written in Fortran. A number of diagnostic tools were built into it, with the outputs in the graphic form. The units of time are normalized so that $T = 1$. For the proof-of-principle purposes of this paper, the simplest time-domain Green function characteristics of the filter system was chosen as shown in Figure 1. Thus, the cooling system is characterized by the gain g and the impulse width $\Delta\tau$ (inverse of the maximum passband frequency). Similarly, in order to avoid the complications of the “unwanted mixing”, the section of the ring between the pickup and the kicker was considered to be isochronous, i.e. the parameter λ there was set to zero. The delay τ_d was matched so that the particle received the self-induced impulse at the kicker at the maximum of the first “hump” in Figure 1. The particles are distributed in momentum x initially in a Gaussian distribution with a unit r.m.s. size σ , while the revolution frequency depends on x as $\omega = 1 + \lambda x$. An example of the output of the correlation function $K(\tau)$ and the corresponding Schottky spectrum $\tilde{S}(\omega)$ for the case of no cooling is given in Figures 2 and 3.

An example of the cooling dynamics with parameters: number of particles $N = 1000$, impulse width $\Delta\tau = .05$, gain $g = .0002$ is shown in Figure 4. There, the r.m.s. momentum spread $\sigma(t)$ is shown as a function of time t , measured in number of time steps. The time step of the mapping in this case is $\tau_0 = .5$. By the end of the cooling period $T_k = 10000\tau_0$ the momentum spread σ is diminished by about 5 times. That large decrease indicates that

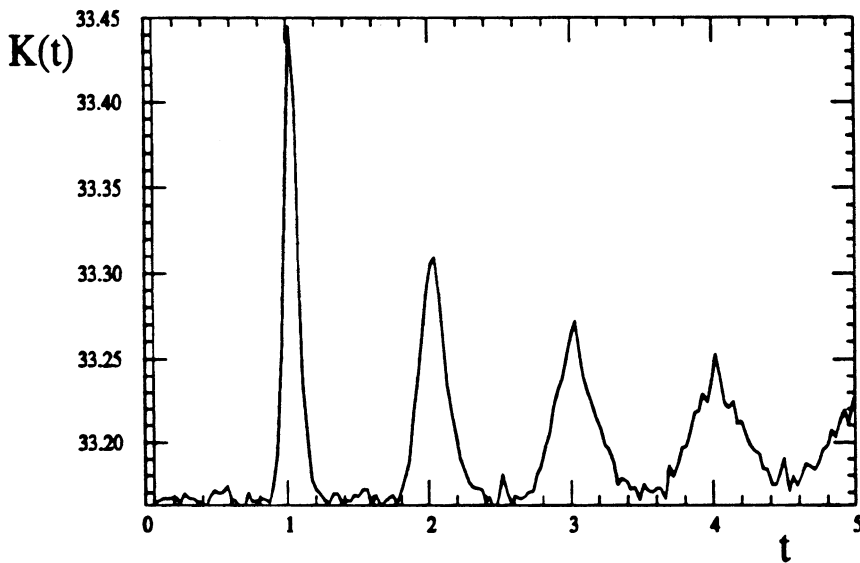


FIGURE 2: An example of the correlation function $K(\tau)$ for number of particles $N=1000$, time step of the mapping $\tau_0=0.765$, nonlinearity $\lambda=0.05$. Schottky computation parameters are $T_s=50$, $T_k=5000\tau_0$, $n_v=30$.

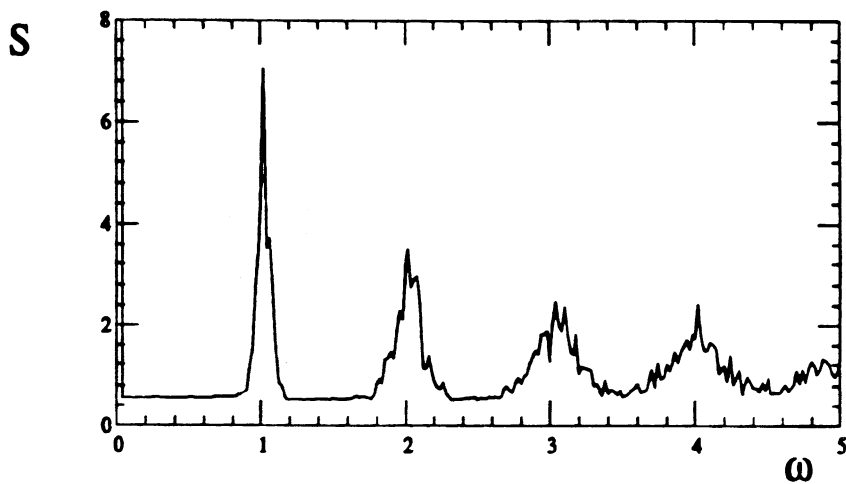


FIGURE 3: Power spectrum $S(\omega)$ for the case of Figure 2.

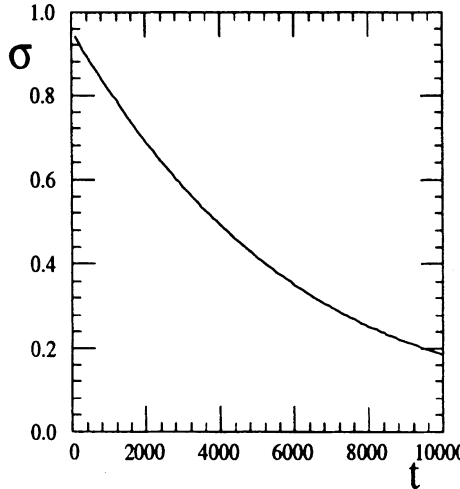


FIGURE 4: Momentum spread σ as a function of time t . Cooling system parameters are $\Delta\tau=.05$, gain $g=.0002$, number of particles $N=1000$, nonlinearity $\lambda=.05$.

the gain g is much smaller than its optimal value (that would provide the fastest cooling). Indeed, for the optimal gain the “suppression factors” ϵ_l equal to $2^{1.5}$ for each band l , so that the momentum spread is not far from the critical value of instability threshold and no big decrease in momentum spread without crossing the threshold is possible.

Two control runs to test the validity of the scaling laws (6) and (8) were made. First, the particle number scaling (6) was tested by simulating the example with 2.5-times less particles ($N = 400$) and 2.5-times higher gain ($g = .0005$) than in the example of Figure 4, all other parameters being the same. When the run time T_k was set at 2.5 times smaller value $T_k = 4000\tau_0$, the curve of the momentum spread versus time $\sigma(t)$ was undistinguishable from the one in Figure 4. The validity of the scaling law (6) tested out thereby perfectly well.

The second test was directed toward the “bandwidth” transformation (8). The impulse width $\Delta\tau$ and the nonlinearity λ were both reduced from the example of Figure 4 by 2.5 times to the values $\Delta\tau = .04$, $\lambda = .02$, while the gain g was increased by a factor 2.5 to the value $g = .0005$. When the run time T_k was set at 2.5 times smaller value than in the example of Figure 4, the curve of the momentum spread versus time $\sigma(t)$ was within a few percent deviation from the curve of Figure 4. The validity of the scaling law (8) tested out thereby as well as one could expect it to.

It should be noted here that since the momentum spread is cooled so much over the run of Figure 4, the test of scaling by comparing the curves $\sigma(t)$ with that of Figure 4 is very convincing, as the cooling rates for different momentum spread values are compared simultaneously.

4 MOMENTUM STACKING

The scaling laws of Section 1 can be implemented to simulate the momentum stacking of antiprotons. Consider the example of Fermilab Accumulator with the parameters:

$$\Delta N = 7 \cdot 10^7 \text{ (number of particles per injection)}$$

$$\Delta t = 2.4 \text{ sec (injection period)}$$

$$f_0 = 0.6 \text{ MHz (revolution frequency)}$$

$$f_{\max} = 2 \text{ GHz, } f_{\min} = 1 \text{ GHz (maximum and minimum frequencies of the stack-tail system passband)}$$

$$\Delta f = 135 \text{ Hz (revolution frequency spread of the stack)}$$

$$t_{\max} = 40 \text{ Hrs (maximum stacking time)}$$

All three transformations (6), (8) and (10) have to be used in order to maximally reduce the number of particles and speed up the simulation. The limiting factors in this approach are the implicit assumptions in the derivation of the FPE (1). The first of these is the “many-particle-per-sample” condition (7). The second one is the absence of the Schottky-band overlap in the rescaled system:

$$\frac{f'_{\max}}{f_0} \frac{\Delta f'}{f_0} < 1 \quad (18)$$

Of all three transformations, only the transformation (10) changes the ratio $f'_{\max} \Delta f' / f_0^2$. Consequently, for the case of Fermilab Accumulator, where that ratio is already close to unity, the scaling parameter k_1 in the transformation (10) can not be made larger than unity.

The third condition for the applicability of the FPE is the smallness of the “decoherence time” $\tau_d = 1/\lambda\sigma_x$ relative to the “cooling time” $\tau_c = \sigma/F(x)$:

$$\frac{\sigma_x}{F(x)} \gg \frac{E_0}{\eta\sigma_x} \quad (19)$$

where σ_x is the e-folding distance (in momentum) of the gain profile, η is the momentum compaction factor $\eta = (\delta f/f)/(\delta p/p)$, E_0 is the injection momentum and $F(x)$ is the “cooling force” (3). The condition (27) is most restrictive near the injection energy since the “cooling force” is maximal in that region. The maximum scaling constant k in the scaling transformation (6) is limited by the condition (19).

The transformations (8) and (10) are applied now by choosing the scaling parameters k_1 and R so as to increase the revolution frequency spread Δf and decrease the bandwidth $W = f_{\max} - f_{\min}$ to numerically convenient values. We choose the new maximum frequency

f'_{\max} from the condition $f'_{\max}/f_0 = W/Rf_0 = 10$. The parameter R is found then to be $R = 330$. The parameter k_1 is chosen on the basis of a preference for a new injection current $J' = \Delta N'/\Delta t'$ of the magnitude:

$$J' = \frac{\Delta N}{f_0 \Delta t} \frac{k_1}{R} = 0.1 \text{ (particles/turn)} \quad (20)$$

This value is deemed optimal in order to have a suitably long tracking time $T_{tr} \approx 5000 - 20000$ turns that would accomodate about 2.5 orders of magnitude of density variation over the stack tail. The parameter k_1 is found then to be $k_1 = .6$ and the rescaled frequency spread becomes $\Delta f'/f_0 = Rk_1\Delta f/f_0 = 0.05$.

The transformation (6) is applied by increasing the gain while keeping both parameters ΔN , Δt and therefore the injection flux constant. That speeds up the evolution of the distribution function $\rho'(x, t) = \rho(x, kt)/k$ (here the distribution ρ is not normalized $\rho = \Psi: N(t), \int \rho dx = N(t)$). The limiting factor to increasing the gain is the condition (19).

For the purpose of the proof-of-principle simulation a simplified model of the stacking system is used, with the purely exponential “pickup sensitivity” dependence $H(x) = H_0 \exp(x/\sigma_x)$ in the range of the dimensionless momentum variable from $x = 0$ (injection) to the $x = -10$. For values of x smaller than -10 , the sensitivity is a linear function of momentum: $H = H_0(x - x_c)/(-10 - x_c) \exp(-10/\sigma_x)$ (x_c is less than -10). That region models the core system, and the core location $x = x_c$ is defined by the condition $H(x) = 0$. The Green function time dependence $\tilde{G}(t)$ was taken to be the same as shown by fat curve in Figure 1. Notice that the integral of the Green function over time has to be zero, since the gain is zero at zero frequency.

Two examples of stacking simulation results are shown in Figures 5 and 6. The width $\Delta\tau$ of the Green function impulses is $\Delta\tau = 0.05$, which approximately corresponds to the maximum passband frequency $f_{\max}/f_0 = 10$. Other parameters are: frequency spread $\Delta f/f_0 = 0.05$, core position $x_c = -10.2$, pickup sensitivity e-folding distance $\sigma_x = 2.1$, injection period $\Delta t = 20$ (turns), injection number of particles $\Delta N = 2$. The plotted graphs are ten successive (equidistant in time) profiles of the base 10 logarithm of the density distribution. In order to improve the statistics of the density representation, each histogram comprises all particles at all time steps within the one-tenth of the total tracking time.

One can see that in the exponential region of the pickup sensitivity $H(x) = H_0 \exp(x/\sigma_x)$ the profiles approach the stationary distribution $\Psi \sim \exp(-x/\sigma_x)$ in accordance with an analytical solution of the FPE that is allowed in this region.¹ Overall, the profiles qualitatively resemble the ones that were obtained for the Accumulator by means of the Van der Meer simulation code, based on the FPE (see, e.g.¹), with about 2 orders of magnitude of density variations in the “tail” part and about one order of magnitude still more in the density variation in the “core” region. The most important conclusion overall is that we are able to reproduce 3 orders of magnitude of the dynamic range of variation of density.

An illustration of the distortions in the density profiles that start emerging when the gain is pushed too high, is given in Figure 6. All parameters are the same as in the case of Figure 5, except for the twice larger gain $H_0 = 0.2$ and twice shorter tracking time $T_{tr} = 12000$

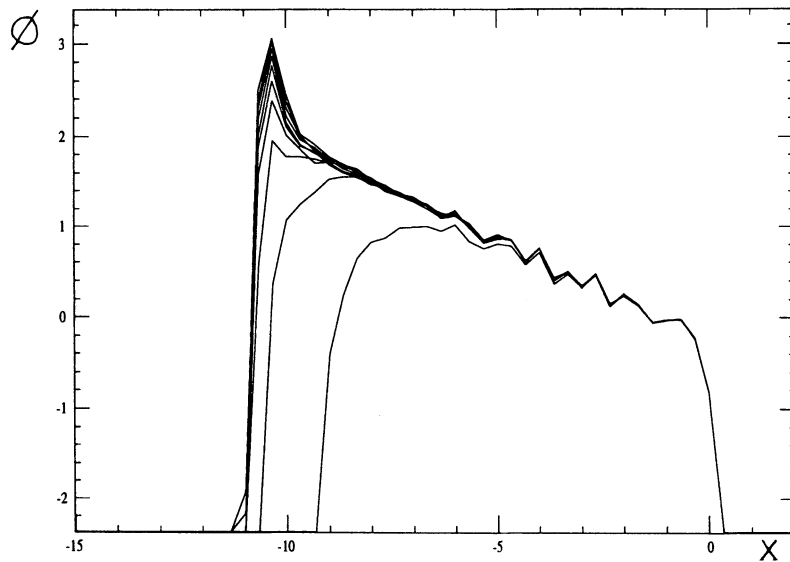


FIGURE 5: 10 Equidistant (in time) logarithmic density $\phi = \log_{10} \rho$ profiles. Tracking time $T_{tr} = 24000$ (turns). Gain strength is defined by $H_0 = 0.1$.

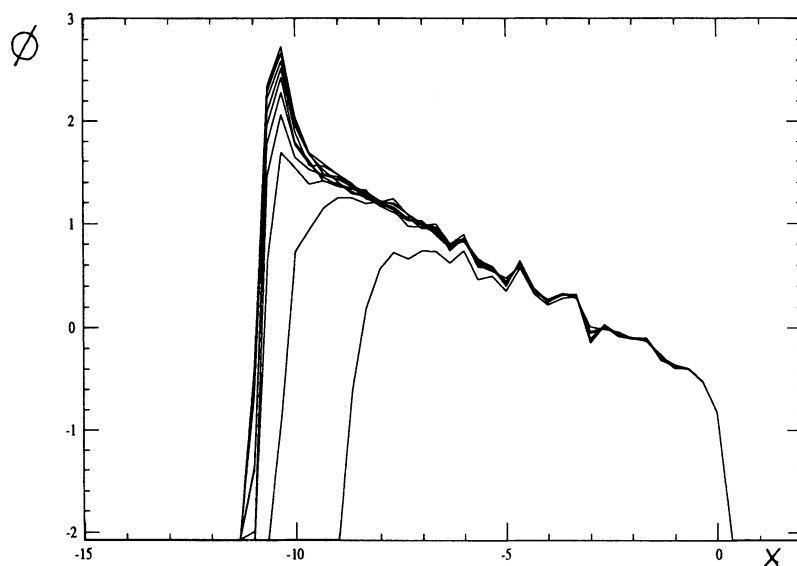


FIGURE 6: 10 Equidistant (in time) logarithmic density $\phi = \log_{10} \rho$ profiles for the parameters of Figure 5, but with a twice higher gain. Tracking time $T_{tr} = 12000$ (turns). Gain strength is defined by $H_0 = 0.2$.

(turns) (so that the profiles should stay invariant if all restrictions (7), (18) and (19) are satisfied). One can notice some differences in the profiles of density even in the region not so close to the injection.

More numerical results are presented in Reference 6.

ACKNOWLEDGEMENTS

I wish to thank V. Visnjic and R. Pasquinelli for a number of useful discussions. The advice of M. Church on the specifics of cooling techniques and the final form and content of the paper was extremely helpful and is gratefully acknowledged.

REFERENCES

1. A.V. Tollestrup, G. Dugan, *Elementary stochastic cooling*. Proc. 1981 SLAC Summer School on Accelerator Physics.
2. V. Visnjic, J. Marriner, *Van der Meer Cooling Simulation Code Manual*. Fermilab, 1992 (unpublished).
3. A. Gerasimov, M. Church. *Macroparticle simulation of antiproton stacking in the Fermilab Accumulator*, to appear.
4. V. Visnjic, *private communication*.
5. J. Bisognano, C. Leemann, *Stochastic cooling*. AIP Conf. Proc., **87**, Fermilab Summer School on Accelerator Physics, 1981.
6. A. Gerasimov, *Macroparticle simulation for stochastic cooling* Fermilab-Pub-94/376, Fermilab, 1994 (unpublished).
7. M. Church, J. Marriner, *Annu. Rev. Nucl. Part. Sci.*, **43** (1993) 253.